Molecular Dynamics Simulation Study of the B-States of Solvated Carbon Monoxymyoglobin

Jianpeng Ma,[†] Shuanghong Huo, and John E. Straub*,[‡]

Contribution from the Department of Chemistry, Boston University, Boston, Massachusetts 02215

Received March 13, 1996. Revised Manuscript Received August 16, 1996[⊗]

Abstract: Classical molecular dynamics simulation is employed to study the photodissociated B-states of carbon monoxymyoglobin. Four independent 10 ps dynamical trajectories of the fully solvated protein, in a box of 2988 water molecules using periodic boundary conditions, were simulated at 300 K starting from the equilibrium deoxymyoglobin structure. Two prototypical protein conformational substates, defined by the conformation of the distal histidine, were sampled from a 1.5 ns trajectory of solvated, room temperature deoxymyoglobin. The structure and ligand vibrational spectral line shapes and frequency shifts were derived from the simulation trajectories. The simulated structure of the ligand−heme complex shows that the ligand is localized under the C-ring of the heme, which is consistent with the low-temperature X-ray crystal structures of the photolyzed state [Schlichting *et al*. *Nature* **1994**, *371*, 808. Teng; Šrajer; Moffat *Nat. Struct. Biol*. **1994**, *1*, 701]. The ligand is found to be parallel to the heme "plane" and confined to a small region displaced from the heme iron in apparent agreement with the low-temperature X-ray crystal structures and room temperature experimental studies [Lim; Jackson; Anfinrud *Science* **1995**, *269*, 962]. Stark shifts in the ligand vibrational frequency, induced by the protein electric field in the heme pocket, are estimated using both atomic point charge models with explicit solvent and finite difference Poisson−Boltzmann calculations. Simulated ligand frequency shifts are compared with those of the experimental spectrum as a test of the accuracy of the simulated electric field in the heme pocket. The magnitudes of the induced ligand frequency shifts are in good agreement with experimental results. The largest contribution to the electric field in the heme pocket is due to the heme and proximal histidines not, as it has often been assumed, the distal histidine. The exact value of the protein electric field experienced by the ligand is well correlated with the conformation of the distal His. The dipole induced in the ligand by the protein electric field is found to make a significant contribution to the total ligand dipole moment and is not necessarily aligned with the ligand bond. The proposal that the ligand "docking site" functions to suppress CO binding is examined.

I. Introduction

The photodissociation and rebinding of ligands in myoglobin (Mb) and hemoglobin provide a rich system for experimental study of kinetics, structure, and energy transfer in biomolecules. The seminal work on the rebinding kinetics of photodissociated carbon monoxide in myoglobin as a function of temperature, pH, and solvent has provided a detailed picture of protein dynamics from picoseconds to milliseconds in time.[1−3] Additionally, computer simulation has shown that a complete description of protein function must include the inherent flexibility and fluctuation of the protein.[4−6] It is likely that the lessons learned from these studies are generally applicable to all proteins. For example, the time scales for fluctuations and transitions ranging from picoseconds to seconds are expected to be present in any protein system, while their detailed relation to function may differ. Further probing of the system by many experimental and theory labs continues using mutants[7] and increasingly precise spectroscopic techniques.[8−12] The intense interest in this system is justified by the possibility that heme protein function (ligand binding and discrimination) and dynamics (ligand binding and vibrational relaxation and dephasing) will be "solved" in all aspects.[13]

Computer simulation of the room temperature, fully solvated protein may be used to address important questions relating to the structure and dynamics of carbon monoxymyoglobin (MbCO), which cannot be resolved unambiguously using existing experimental methods. In this study, we use molecular dynamics simulation to explore the protein structure and ligand dynamics of the B-states. The simulations were designed to address a number of important questions which we enumerate in the context of the following background material.

A. Short Time Dynamics Following Photolysis. The infrared spectrum of the carbon monoxide stretch ν_{CO} had been measured for the ligand bound to the heme (A-states) and dissociated (B-states). In MbCO, Fourier transform infrared spectroscopy has isolated distinct lines for ν_{CO}, known as the A-states.[14] The frequency shifts are independent of pH, and the widths and areas are temperature sensitive above 180 K.

[†] Current address: Department of Chemistry, Harvard University, Cambridge, Massachusetts 02138.

[‡] Alfred P. Sloan Research Fellow (1995−1997).

[⊗] Abstract published in *Advance ACS Abstracts*, February 15, 1997.

(1) Ansari, A.; Berendzen, J.; Braunstein, D.; Johnson, J. B.; Ormos, P.; Sauke, T. S.; Scholl, R.; Schulte, A. *Biophys. Chem*. **1987**, *26*, 337.

(2) Austin, R. H.; Beece, K. W.; Eisenstein, L.; Fauenfelder, H.; Gunsalus, I. C. *Biochemistry* **1975**, *14*, 5355.

(3) Campbell, B. F.; Chance, M. R.; Friedman, J. M. *Science* **1987**, *238*, 373.

(4) Case, D.; Karplus, M. *J. Mol. Biol*. **1979**, *132*, 343.

(5) Elber, R.; Karplus, M. *J. Am. Chem. Soc*. **1990**, *112*, 9161.

(6) Kottalam, J.; Case, D. A. *J. Am. Chem. Soc*. **1988**, *110*, 7690.

(7) Olson, J. S.; Matthews, A. J.; Rohlfs, R. J.; Springer, B. A.; Egeberg, K. D.; Sligar, S. G.; Tame, J.; Renaud, J.-P.; Nagai, K.; Poyart, C.; Lecarpentier, Y.; Astier, R.; Antonetti, A. *Nature* **1988**, *336*, 265.

(8) Anfinrud, P. A.; Han, C.; Hochstrasser, R. M. *Proc. Natl. Acad. Sci. U.S.A.* **1989**, *86*, 8387.

(9) Lim, M.; Jackson, T. A.; Anfinrud, P. A. *J. Chem. Phys*. **1995**, *102*, 4355.

(10) Lim, M.; Jackson, T. A.; Anfinrud, P. A. *Science* **1995**, *269*, 962.

(11) Hill, J. R.; Tokmakoff, A.; Peterson, K. A.; Sauter, B.; Zimdars, D.; Dlott, D. D.; Fayer, M. D. *J. Phys. Chem*. **1994**, *98*, 11213.

(12) Owrutsky, J. C.; Li, M.; Locke, B.; Hochstrasser, R. M. *J. Phys. Chem*. **1995**, *99*, 4842.

(13) Springer, B. A.; Sligar, S. G.; Olson, J. S.; Phillips, G. N., Jr. *Chem. Rev*. **1994**, *94*, 699.

S0002-7863(96)00825-6 CCC: $14.00

In photolyzed Mb*CO, the dissociated carbon monoxide ligand is observed to stay in the pocket during the formation of the B-state frequency shifts implying that the frequency shifts are induced by the charges and conformation of the protein heme pocket. Infrared spectroscopy of the carbon monoxide stretching frequency following photodissociation shows three distinct values of ν_{CO} (with B_0 seen only at cryogenic temperatures).[15] The shifts in ν_{CO} correspond to three conformations of the carbon monoxide−myoglobin system known as the B-states. The early protein dynamics following photodissociation have been studied using time-resolved femtosecond spectroscopy,[16] which shows the formation of the deoxy species within 350 fs.[16,17] Computer simulation of the photodissociation of carbon monoxide from hemoglobin has demonstrated the fast relaxation of the heme within 50−150 fs.[18] There has been some success in defining the transient events of the ligand dynamics following photodissociation using ultrafast subpicosecond spectroscopy.[8,16] These studies have been directed at characterizing the time scale for formation of the B-states of the dissociated carbon monoxide ligand in hemoglobin. The B-states are observed within 300−500 fs of photolysis, and the spectrum does not change significantly between 500 and 1 ns.[8] In fact, up to 1 ns after photolysis, greater than 85% of the ligand remains in the heme pocket.[19]

(1) What is the mechanism of rotational relaxation for the unbound CO ligand in the heme pocket, and how does the simulated rotational dynamics compare with that inferred from experimental IR line shapes? How does the relaxation depend on the structure of the heme pocket?

B. Origins of Frequency Shifts in MbCO and Mb*CO. It is well established that the observed ligand frequency shifts of the A-states correspond to local changes in the conformation or protonation state of residues forming the heme pocket rather than global changes in the protein conformation.[13,20,21] Alben *et al*. demonstrated that B_1 and B_2 may interconvert at 20.1 K, leading to an estimate of the barrier to interconversion between the states of 0.9 kcal/mol.[15] Key interactions with the heme and distal histidine are expected to play an important role in inducing the frequency shifts observed in the A- and B-states.[20]

For the A-states, experiments on distal His → Gly mutants show one A-state, indicating the conformational and ionization states of the distal His are the origin of the A-state frequency shifts.[22] Low-temperature experiments show a blue-shifted B-state which disappears in the His → Gly mutant. However, structural changes in the pocket may be considerable. Additionally, the mutant spectra show only two B-states (2137 and 2125 cm^{-1}). Together, these observations confirm that His64 contributes to the frequency shifts of the different B-states.

Dykstra and co-workers[21] have analyzed in detail the ν_{FeC} and ν_{CO} frequency shifts of the A-states in terms of the degree of π back-bonding of π^* orbitals of CO to iron d orbitals, and the variation in this interaction due to local fields generated by the surrounding residues. Augspurger, Dykstra, and Oldfield have studied the effects of an external electric field (and field gradient) on carbon monoxide using high-level *ab initio* calculations.[23] Their study provides a clear picture of the effects which determine frequency shifts in carbon monoxide in the presence of an external field that would be experienced in a protein. Given an accurate representation of the electrostatic environment in the protein, it should be possible to quantitatively predict the vibrational frequency shift.

The relative importance of steric and electrostatic effects for inducing frequency shifts in the Fe−CO structure has been carefully analyzed by Ray *et al*.;[24] they have concluded that the substates for solvated MbCO are determined by electrostatic interactions with the distal His in its $H_{\delta 1}$ (A_3) and $H_{\epsilon 2}$ ($A_{1,2}$) tautomeric forms. In an examination of 41 recombinant myoglobins, Li *et al*.[25] concluded that the ν_{CO} of the A-states is determined by electrostatic interactions where the distal His plays a central role. Work by Sakan *et al*.[26] showed that the ν_{FeCO} band measured by resonance Raman was correlated with the electrostatic character (measure by a "hydropathy" index) but not with the assumed steric interactions (or physical size of the particular distal mutant residue).

The first molecular dynamics study of the effects of the protonation state of the distal His on ligand structure and dynamics was completed by Straub and Karplus who examined the $H_{\delta 1}$ tautomer and the charged form His^+ (dominant at low pH).[27] The charged form was found to have the distal His^+ flipped out into the solvent in agreement with the "open" conformation proposed by Champion and co-workers[28] and subsequently seen in the low-pH crystal structure.[29] Jewsbury and Kitagawa[30] examined distal His−CO interactions in MbCO focusing on the two distal His tautomers which, based on their calculations, they assigned to the $A_{1,2}$- ($H_{\delta 1}$) and A_3- ($H_{\epsilon 2}$) states. This assignment is the opposite of that proposed by Ray *et al*.[24] While details are uncertain, existing experimental and computational evidence conclusively points to the importance of electrostatics in determining the frequency shifts of ν_{CO} in the different A- and B-states and the crucial role of the distal His64 in determining the electrostatic potential in the heme pocket through its protonation state and conformation.

(2) Which portions of the protein make the largest contributions to the electric field in the heme pocket, and how does the simulated electric field compare with previous estimates assumed to be dominated by the distal histidine?

(3) How does the electric field computed for the simulated solution structure compare with that calculated for the low-temperature X-ray structure?

(14) Steinbach, P. J.; Ansari, A.; Berendzen, J.; Braunstein, D.; Chu, K.; Cowen, B. R.; Ehrenstein, D.; Frauenfelder, H.; Johnson, J. B.; Lamb, D. C.; Luck, S.; Mourant, J. R.; Nienhaus, G. U.; Ormos, P.; Philipp, R.; Xie, A.; Young, R. D. *Biochemistry* **1991**, *30*, 3988. Mourant, J. R.; Braunstein, D. P.; Chu, K.; Frauenfelder, H.; Nienhaus, G. U.; Ormos, P.; Young, R. D. *Biophys. J*. **1993**, *65*, 1496. Braunstein, D. P.; Chu, K.; Egeberg, K. D.; Frauenfelder, H.; Mourant, J. R.; Nienhaus, G. U.; Ormos, P.; Sligar, S. G.; Springer, B. A.; Young, R. D. *Biophys. J*. **1993**, *65*, 2447.

(15) Alben, J. O.; Beece, S. F.; Bowne, F.; Doster, W.; Eisenstein, L.; Frauenfelder, H.; Good, D.; McDonald, J. D.; Marden, M. C.; Moh, P. P.; Reinisch, L.; Reynolds, A. H.; Shyamsunder, E.; Yue, K. T. *Proc. Natl. Acad. Sci. U.S.A.* **1982**, *79*, 3744.

(16) Martin, J. L.; Migus, A.; Poyart, C.; Lecarpentier, Y.; Astier, R.; Antonetti, A. *Proc. Natl. Acad. Sci. U.S.A.* **1983**, *80*, 173.

(17) Petrich, J. W.; Poyart, C.; Martin, J. L. *Biochemistry* **1988**, *27*, 4049.

(18) Henry, E. R.; Levitt, M.; Eaton, W. A. *Proc. Natl. Acad. Sci. U.S.A.* **1985**, *82*, 2034.

(19) P. A. Anfinrud, private communication.

(20) Fiamingo, F. G.; Alben, J. O. *Biochemistry* **1985**, *24*, 7964.

(21) Oldfield, E.; Guo, K.; Augspurger, J. D.; Dykstra, C. E. *J. Am. Chem. Soc*. **1991**, *113*, 7537.

(22) Braunstein, D.; Ansari, A.; Berendzen, J.; Cowen, B. R.; Egeberg, K. D.; Frauenfelder, H.; Hong, M. K.; Ormos, P.; Sauke, T. B.; Scholl, R.; Schulte, A.; Sligar, S. G.; Springer, B. A.; Steinbach, P. J.; Young, R. D. *Proc. Natl. Acad. Sci. U.S.A.* **1988** , *85*, 8497.

(23) Augspurger, J. D.; Dykstra, C. E.; Oldfield, E. *J. Am. Chem. Soc.* **1991**, *113*, 2447.

(24) Ray, G. B.; Li, X.-Y.; Ibers, J. A.; Sessler, J. L.; Spiro, T. G. *J. Am. Chem. Soc*. **1994**, *116*, 162.

(25) Li, T.; Quillin, M. L.; Phillips, G. N., Jr.; Olson, J. S. *Biochemistry* **1994**, *33*, 1433.

(26) Sakan, Y.; Ogura, T.; Kitagawa, T.; Fraunfelter, F. A.; Mattera, R.; Ikeda-Saito, M. *Biochemistry* **1993**, *32*, 5815.

(27) Straub, J. E.; Karplus, M. *Chem. Phys*. **1991**, *158*, 221.

(28) Morikis, D.; Champion, P. M.; Springer, B. A.; Sligar, S. G. *Biochemistry* **1989**, *28*, 4791.

(29) Quillin, M. L.; Arduini, R. M.; Olson, J. S.; Phillips, G. N., Jr. *J. Mol. Biol*. **1993**, *234*, 140.

(30) Jewsbury, P.; Kitagawa, T. *Biophys. J*. **1994**, *67*, 2236.

(4) How do estimates of the electric field generated by atomic models using explicit solvent compare with estimates based on continuum electrostatics?

(5) What are the predicted ligand frequency shifts based on the computed values of the protein electric field in the heme pocket? How do the predicted shifts compare with the experimentally determined values?

C. Discrimination in Ligand Binding Affinity. There is a significant reduction in the CO heme binding affinity in the protein relative to a protoheme.[13] Meanwhile, the protein environment has much less influence on the binding affinity of O_2.[31] This problem has a long history, and it is still in debate today. One scenario attributed the affinity discrimination to steric effects in the heme pocket.[32−34] Repulsion between the CO and heme pocket residues was proposed to disfavor the binding of the CO to the heme. Support for this proposal came from a tilted CO conformation obtained from X-ray measurement on the $P2_1$ crystal form.[34] Experimental results on the $P6$ crystal form and in solution[10,24,29,35,36] seem to reveal that the CO prefers a relatively vertical conformation in the bound state (A-states). This is supported by X-ray crystal structures from Quillin *et al*. for the $P6$ crystal form which show the Fe−C−O complex to be less bent than in the $P2_1$ crystal structure (although not linear). Therefore the ligand tilt, significant in the $P2_1$ crystal, can be influrenced by the crystal form.[29]

Regardless of the importance of steric effects, the results of mutation experiments[25,26,29] indicate that the decisive interactions between the CO ligand and key residues such as the distal histidine are electrostatic.[21,24,25] Pauling made the first such proposal, identifying hydrogen bonding to the O_2 ligand (but not CO) by the distal His.[37]

With the former explanation of diminished CO binding in question, an intriguing hypothesis on the mechanism of ligand discrimination in myoglobin has been proposed by Lim, Jackson, and Anfinrud on the basis of their ultrafast IR spectroscopic data.[9,10] In their mechanism, following photolysis the CO ligand is localized in a heme pocket "docking site" in which the dissociated CO ligand is parallel to the heme plane. They proposed that the difference in binding rate between CO and O_2 is due to the unfavorable orientation of CO on rebinding. The parallel CO conformation in the photodissociated state (with the distances Fe−C 4.14 Å and Fe−O 3.60 Å) was observed in the recent X-ray crystal structure of photodissociated Mb*CO obtained at ultra low temperature.[38] A similar study at 40 K reported that the angle of the ligand with respect to the heme plane normal was close to 90°.[39] However, at these low temperatures there is frustrated relaxation in the X-ray structure of Mb*CO—the heme iron moves only partially out-of-plane. Whatever the true reason is for the discrimination of ligand binding affinity by the protein, an important conclusion of this recent work is that the real mechanism can only be understood in terms of a detailed picture of the structure and dynamics of the A- and B-states.

(6) What are the room temperature, solution structures of the B-states of MbCO, and how do those structures compare with low-temperature X-ray crystal structures of Mb*CO?

(7) How does the presence of the ligand "binding site" effect the barrier to ligand rebinding?

These questions define the focus of our study. In the next section, we describe our simulation model and the computational methods.

II. Methodology

A. Computational Model and Potentials. The starting point for our computational study was a 1.5 ns equilibrium dynamic trajectory of fully solvated, neutral pH condition, deoxymyoglobin at 300 K.[40] Analysis of this 1.5 ns trajectory provided starting configurations for our study of the B-states of MbCO and insight into conformational fluctuations in the heme pocket. All simulations were performed using a modified version 23 CHARMM program on the Cray C90 at the Pittsburgh Supercomputing Center. The protein potential energy function was modeled using the version 19 CHARMM empirical energy function with a user subroutine for treating the ligand model.[41] The solvent was treated using the TIP3P three-site rigid water model of Jorgensen and co-workers.[42] The system was constructed using periodic boundary conditions with a rectangular cell of dimension 56.570 Å × 56.570 Å × 37.712 Å including the myoglobin protein, ligand, and 2988 water molecules. The nonbonded potential was truncated by a 9.25 Å shifting function. The distance for the outer sphere cutoff of the neighbor list, and the image update was 10.25 Å.

The carbon monoxide molecule was simulated using a three-site model developed by Straub and Karplus.[27] The RRKR bond-stretching potential of Huffaker was employed.[43−45] The generalized three-site model consists of Lennard−Jones sites and point charges on the carbon and oxygen nuclei and a point charge on the center-of-mass. The model was fit to give good agreement with experimental dipole and quadrupole moments, the experimental lattice constant and sublimation energy for the α − CO crystal, and *ab initio* quantum mechanical energies calculated for carbon monoxide interacting with water, methanol, formamide, and imidazole, as well as the CO hydration free energy.[27]

Accurate calculation of the ligand infrared spectrum depends on a reliable estimate of the ligand dipole moment. We have included to first order the dipole induced in the polarizable CO by the electric field of the protein and solvent. The dipole moment of CO in myoglobin can be approximated as $\vec{\mu} = \vec{\mu}_0 + \vec{\mu}_{\mathrm{ind}}$, which is a sum of the permanent dipole, $\vec{\mu}_0$, and the dipole induced by the external electric,[45] $\vec{\mu}_{\mathrm{ind}} = \overleftrightarrow{\alpha}\cdot\vec{E}$, where $\vec{E}$ is the electrostatic field of the surrounding protein and solvent. It is known that charge redistribution accompanies molecular vibrations in the CO molecule. However, changes in the dipole and quadrupole moments due to bond length fluctuations were found to be insignificant corrections to the properties of interest in this work.[46]

Due to the small polarizability of the CO molecule, we ignore self-consistent polarization which we expect to lead to a small correction to $\vec{E}$. There is the additional complication that the CHARMM force field includes polarization, to some extent, in the choice of partial charges (as for the TIP3P water model). Therefore, it is not a simple matter to add even a constant atomic polarizability without reparameterizing the force field. As we will see, the induced dipole $\vec{\mu}_{\mathrm{ind}}$ is not large in an absolute sense, but it is significant compared with the permanent dipole $\vec{\mu}_0$ of the CO.

The polarizability tensor of carbon monoxide is known from experiments which measure the polarization light scattering in carbon

(31) Antonini, E.; Brunori, M. *Hemoglobin and Myoglobin in their Reactions With Ligands*; North-Holland: London, 1971.
(32) Collman, J. P.; Brauman, J. I.; Halbert, T. R.; Suslick, K. *Proc. Natl. Acad. Sci. U.S.A.* **1976**, *73*, 3333.
(33) Case, D. A.; Karplus, M. *J. Mol. Biol.* **1978**, *123*, 697.
(34) Kuriyan, J.; Wilz, S.; Karplus, M.; Petsko, G. A. *J. Mol. Biol.* **1986**, *192*, 133.
(35) Ösapay, K.; Theriault, Y.; Wright, P. E.; Case, D. A. *J. Mol. Biol.* **1994**, *244*, 183.
(36) Ivanov, D.; Sage, J. T.; Keim, M.; Powell, J. R.; Asher, S. A.; Champion, P. M. *J. Am. Chem. Soc.* **1994**, *116*, 4139.
(37) Pauling, L. *Nature* **1964**, *203*, 182.
(38) Schlichting, I.; Berendzen, J.; Phillips, G. N., Jr.; Sweet, R. M. *Nature* **1994**, *371*, 808.
(39) Teng, T.-Y.; Šrajer, V.; Moffat, K. *Nat. Struct. Biol.* **1994**, *1*, 701.
(40) C. L. Brooks, III, unpublished results.
(41) Brooks, B. R.; Bruccoleri, R. D.; Olafson, B. O.; States, D. J.; Swaminathan, S.; Karplus, M. *J. Comput. Chem.* **1983**, *4*, 187.
(42) Jorgensen, W. L.; Chandrasekhar, J.; Madura, J. D.; Impey, R. W.; Klein, M. L. *J. Chem. Phys.* **1983**, *79*, 926.
(43) Huffaker, J. N. *J. Chem. Phys.* **1988**, *64*, 3175.
(44) Nesbitt, D. J.; Hynes, J. T. *J. Chem. Phys.* **1982**, *77*, 2130.
(45) Berens, P. H.; Wilson, K. R. *J. Chem. Phys.* **1981**, *74*, 4872.
(46) The experimental dipole moment derivative of carbon monoxide is −3.1 D/Å which is substantial considering that the equilibrium dipole moment is only 0.11 D. Within the atomic nuclear point charge model it is not possible to reproduce the dipole moment derivative without changing the charges as a function of the internuclear distance.

monoxide gas. The polarizability can be expressed in terms of the parallel $\alpha_{\|}$ and perpendicular $\alpha_{\perp}$ components and the mean polarizability $\alpha = (\alpha_{\|} + 2\alpha_{\perp})/3$. The experimental values are $\alpha = 1.97$ Å^3 and $\alpha_{\|} - \alpha_{\perp} = 0.53$ Å^3.[47] The procedure for rotating the electric field into the ligand frame of reference is described in detail elsewhere.[48]

B. Initial Coordinates, Conformational Substates, and Dynamics Protocol. It is important to perform calculations from independent starting configurations to test the validity of our results. However, is it reasonable to simulate dissociated B-states of MbCO starting from the deoxymyoglobin (deoxy-Mb) structure? There is spectroscopic evidence that the heme group relaxes within 350 fs from the planar conformation, corresponding to the bound ligand, to the domed pentacoordinate conformation, when the ligand is dissociated.[49] Tertiary conformational changes in the protein have been found to follow ligand photodissociation in molecular dynamics simulations. These changes consist of helix shifts and require 10−50 ps to complete. Most of the configurational relaxation of photolyzed MbCO appears to be completed in 1 ns, while 10 ns is required for complete relaxation.[50,51] The IR band for the B_1-state moves nonexponentially in frequency for up to 10 ns following photolysis, but it is stable thereafter.[19] However, the effect of the time dependent frequency shift is minor in magnitude and the B_1- and B_2-states remain clearly resolved. Therefore, while tertiary conformational changes taking place on a nanosecond time scale are coupled to the frequency shift induced in the spectra of the unbound ligand, simulation of the ligand in the relaxed state of the protein provides a good model of the dissociated ligand 10 ns or more following photolysis at room temperature.

It is the room temperature, solvated state of the protein that is of interest to us. As much as 10 ns of dynamics is required from the time of photodissociation until a representative structure of the equilibrium B-state is achieved. Therefore, it was not feasible for us to simulate the solvated B-states of MbCO starting from the equilibrium solvated state of MbCO. It is even more forbidding to start from the low-temperature X-ray crystal structure of the photolyzed state of MbCO or the X-ray crystal structure of MbCO. In each case, equilibration of the solvated state of MbCO would be required before the photodissociation is simulated and equilibration is achieved. However, by initiating the simulation from the crystal structure of deoxy-Mb, it is possible to obtain an apparently equilibrated state of solvated deoxy-Mb. After introduction of the CO ligand, with minimal perturbation to the protein structure (the heme remaining in the domed, pentacoordinated state), an equilibrated, solvated state of the dissociated MbCO is obtained. This procedure avoids the simulation of the photolysis step and the 10 ns required for the heme and protein relaxation. For this reason, we determined that the solvated deoxy-Mb structure was the best starting point for our simulation study of the dissociated CO ligand in the room temperature, solvated protein−the B-states of solvated carbon monoxymyoglobin.

We have analyzed the 1.5 ns trajectory of deoxy-Mb in water generated by Brooks and co-workers.[52] Using snapshots from this trajectory, we have been able to generate independent starting configurations for our simulations of the B-states of MbCO as well as explore the equilibrium fluctuations in the distal pocket and His64 ($H_{\delta 1}$ tautomer) conformation.

In Figure 1, the time series of the dihedral angle $C_\alpha C_\beta C_\gamma N_{\delta 1}$ of distal histidine along the 1.5 ns trajectory is presented. One can see that the fluctuations of this dihedral angle are usually restricted to two ranges with infrequent transitions between ranges. One range is centered between 60° and 70° and is visited infrequently, while the second and dominant range is centered between −60° and −70°. The former corresponds to a state in which the $H_{\delta 1}$ of His64 is pointing toward the solvent (outward), and the latter corresponds to that same hydrogen

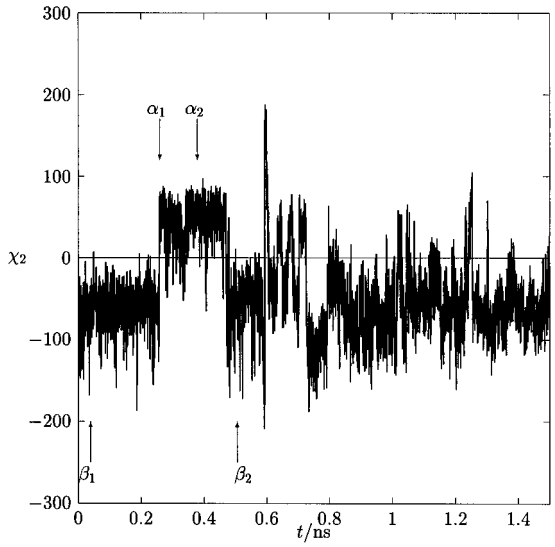

Figure 1. The time series of the χ_2 ($C_\alpha-C_\beta-C_\gamma-N_{\delta 1}$) dihedral angle of the distal His64 for the 1.5 ns equilibrium dynamical trajectory of solvated deoxymyoglobin. Two domains of the χ_2 angle are visible. The points at which the initial conditions of the four trajectories were sampled are indicated. The protein "substates" correspond to outward- (α) and inward- (β) pointing distal His which correlate with greater (open) and more restricted (closed) free volumes in the heme pocket, respectively.

pointing toward the heme pocket (inward). It is clear from the plot that this dihedral angle spends a majority of time in the inward pointing state. We regard these two His64 conformers as markers of the dominant heme pocket conformational states at the neutral pH condition of our simulation. At low pH, experimental results[53] reveal that the distal histidine could be repelled into the solvent. Along the entire 1.5 ns trajectory, the distal histidine mainly stays inside the heme pocket. We found no significant transition of the dihedral angle $CC_\alpha C_\beta C_\gamma$ at neutral pH.

From the 1.5 ns dynamical trajectory of deoxymyoglobin, we selected four snapshots (two with each of two different distal histidine conformations) as our initial configurations for our dynamical simulation of photolyzed Mb*CO. These initial states are separated by over 100 ps of room temperature dynamics so that they are relatively independent. The CO bond was initially placed along the line of His93 $N_{\epsilon 2}$−Fe in the heme pocket. After the placement of the CO molecule, the steepest descent method was employed to minimize the energy of the CO structure with the protein and solvent atoms fixed. We have found that adding the CO to the heme pocket of deoxy-Mb is a minor perturbation to the protein structure. It appears that the resulting protein/ligand structure can be considered to be as representative of the equilibrium ensemble of B-states of carbon monoxymyoglobin as the parent deoxy-Mb structure from which it was derived.

The simulations were conducted at a temperature of 300 K. The SHAKE algorithm[54] was employed to keep the bond lengths of the water molecules and all other bonds involving a hydrogen atom fixed. The integration time step was 0.5 fs using the velocity Verlet integrator.[55] The nonbonded pair list and image pair list were updated every 10 steps. Initial velocities were sampled from a Maxwell distribution at 300 K. For the first picosecond, the temperature of the system was unconditionally scaled to 300 K every 0.05 ps to equilibrate the system. After that, another 4 ps of dynamics was run with a temperature window of 300 ± 5 K. The temperature was scaled only when the temperature moved outside the window. We noticed that over the entire 4 ps equilibration period the velocities were rescaled at most two times. This indicates that the trajectory was well equilibrated after the first 5 ps equilibration phase and the preceding extended

(47) Bridge, N. J.; Buckingham, A. D. *Proc. R. Soc. London* **1966**, *295*, 334.
(48) Berne, B. J.; Pecora, R. *Dynamic Light Scattering*; Wiley-Interscience: New York, NY, 1976.
(49) Moore, J. N.; Hansen, P. A.; Hochstrasser, R. M. *Proc. Natl. Acad. Sci. U.S.A.* **1988**, *85*, 5062.
(50) Lim, M.; Jackson, T. A.; Anfinrud, P. A. *Proc. Natl. Acad. Sci. U.S.A.* **1993**, *90*, 5801.
(51) Jackson, T. A.; Lim, M.; Anfinrud, P. A. *Chem. Phys.* **1994**, *180*, 131.
(52) C. L. Brooks, III, unpublished results.
(53) Yang, F.; Phillips, G. N., Jr. *J. Mol. Biol.* **1996**, *256*, 762.
(54) van Gunsteren, W. F.; Berendsen, H. J. C. *Mol. Phys.* **1977**, *34*, 1311.
(55) Swope, W. C.; Andersen, H. C.; Berens, P. H.; Wilson, K. R. *J. Chem. Phys.* **1980**, *72*, 4350.

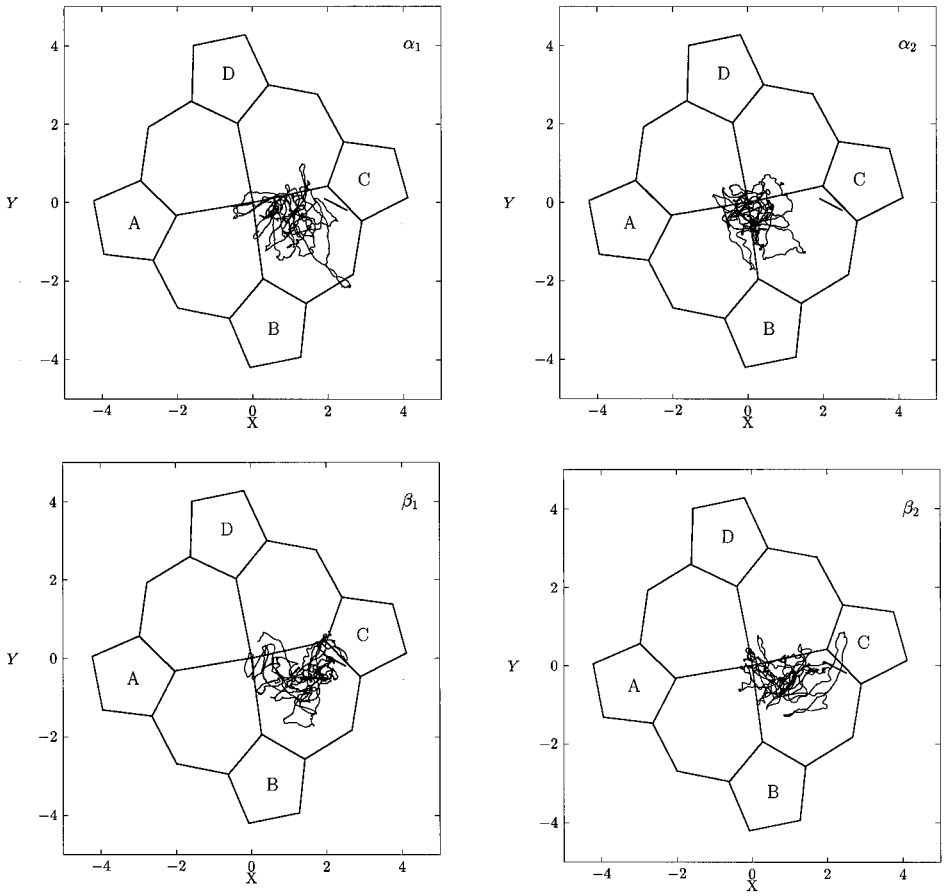

Figure 2. The projection of CO ligand center-of-mass motion on the heme plane. The heme frame of reference was defined by a least squares fit of the 24 heavy atoms of the heme to a nonrotating plane. The heavy straight line represents the projection of the ligand position from the X-ray crystal structure of photolyzed Mb*CO at liquid helium temperature.[38] The results are for the four trajectories noted in Figure 1.

equilibration of the parent deoxy-Mb system. This rapid equilibration is consistent with experimental evidence which indicates that the presence of the CO ligand is a small perturbation to the structure of the protein.[34] After the equilibration, we generated four 10 ps trajectories using the three-site CO model. Two trajectories started from configurations with the distal histidine pointing outward (α) and two trajectories started with an inward-pointing (*β*) distal His.

We omit statistical averages over multiple trajectories since the relative weights of the prototypical α and *β* substates are unknown. Over the 1.5 ns trajectory (Figure 1) the *β* (inward-pointing His64) conformation appears to be approximately four times as probable as the α (outward-pointing His64) conformation. Transitions between these substates appear to be infrequent, and an accurate weight cannot be derived from the 1.5 ns run. A longer run, or the use of biased sampling techniques,[56] must be employed to determine accurate equilibrium substate probabilities.

III. Results and Discussion

A. Room Temperature Structure of the B-States of MbCO. During the 10 ps dynamics, we computed various dynamical properties of the CO ligand. In Figure 2a, we present the projection of the trajectory of the CO center-of-mass on the least squares fitted heme plane defined by the 24 heavy atoms of the heme ring. The result indicates that during the 10 ps dynamics the range of motion of the CO ligand inside the heme pocket is restricted to a region close to the binding site, but for a majority of the time, the position of the ligand is not on top of the iron binding site. The CO motion is localized between the heme B- and C-rings. In the α (outward-pointing distal His) trajectories, the ligand appears to have significantly more motion than in the *β* trajectory. This is consistent with a previous study of the free volume in the heme pocket which investigated the role of the distal His conformation on ligand dynamics.[27]

The crystal structure of photolyzed carbon monoxymyoglobin studied by Schlichting *et al.*[38] shows that the CO ligand is localized at a position under the C-ring of the pyrrole. Considering the fact that the crystal structure represents an average, liquid helium temperature structure, our simulation results are in qualitative agreement. Further, they indicate that the bias of the ligand distribution toward the C-ring is preserved at room temperature.

To investigate the conformation of CO inside the heme pocket, we studied the orientational distribution of CO ligand from our simulation. In Figure 3, we present the distribution function of the angle between the CO bond vector (pointing from the C to the O) and heme normal vector. The average of this angle is 103.3° for the *β* trajectories and 108.1° for the α trajectory. This indicates that the CO ligand is indeed maintaining, on average, a parallel conformation to the heme plane in both the α and *β* trajectories. The distribution of this angle is fairly broad indicating that the motion is moderately hindered. The angular distribution of the α conformation with the distal His pointing outward is broader than that of the *β* conformation with the inward-pointing distal His. This indicates that the mobility of the CO in the heme pocket of the α (outward) conformation is greater than that in the *β* (inward) conformation as one would expect based on the free volume in the heme pocket. The data in Table 1, which show that the distances from the C and O atoms to the Fe atom are on average slightly greater over the α trajectories, support this conclusion. The

(56) Hodel, A.; Simonson, T.; Fox, R. O.; Brünger, A. T. *J. Phys. Chem.* **1993**, *97*, 3409.

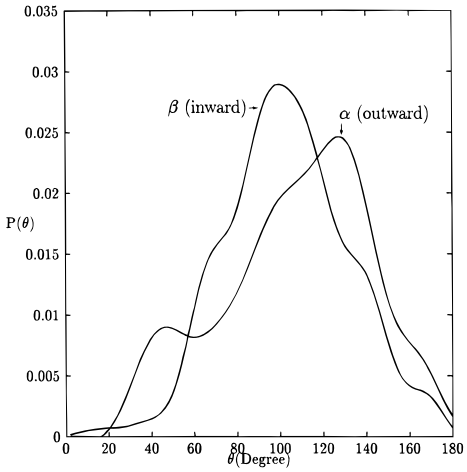

Figure 3. The angular distribution of the CO bond relative to the heme normal. The distribution is peaked near 100° in the β (inward) trajectory and 135° in the α (outward) trajectory. The β trajectories show the CO to be on average more nearly perpendicular to the heme normal compared with the α trajectories. The distribution is fairly broad indicating that rotational motion is moderately hindered.

Table 1. Structure of Photolyzed Carbon Monoxymyoglobin by Simulation and Experiment

				X-ray	
	α[a]	β[a]	IR[9]	ref 38	ref 39
IR angle (deg)[b]	108.1	103.3	90	91	∼65
CO bend angle (deg)[c]				111	129
Fe−C (Å)	4.54	4.46		4.14	
Fe−O (Å)	4.46	4.16		3.60	
O−$N_{\epsilon 2}$ (His 64) (Å)	6.36	5.21		3.90	

[a] Averages computed over the four trajectories. [b] Angle between the CO ligand bond and the normal to the least squares fit to the heme plane. [c] Angle between the Fe, the nearer, and the farther of the two ligand atoms.

motion of the CO molecule in the heme pocket is anisotropic in space with a bias toward the parallel orientation. This result provides support for the recent proposal of Lim, Jackson, and Anfinrud that the dissociated CO is localized at room temperature in a "binding site" where the ligand is displaced below the B- and C-rings of the heme and is biased to be parallel to the plane of the heme. Table 1 provides a summary of the simulated structure compared with experimentally derived structures.

B. Dipole Orientational Correlation Functions and Vibrational Line Shapes. In Figure 4 we present the dipole orientational correlation function calculated for the α and β trajectories. The data are shown together with the orientational correlation function of a free rotor at 300 K. One can see from these two curves that the dipole orientational correlation function of CO has significantly different features in the protein environment and gas phase. The rotational motion of the CO ligand inside the heme pocket is hindered as was predicted using computer simulation by Straub and Karplus[27] and confirmed experimentally by Lim, Jackson, and Anfinrud.[9] There is a longer average distance between the CO center-of-mass and the heme plane for the α (outward His) trajectory (Table 1). This is correlated with the greater ligand mobility in the α conformational substate.

Note that when the dipole moment is decomposed as $\vec{\mu} = \vec{\mu}_0 + \vec{\mu}_{\mathrm{ind}}$, the dipole correlation function can be decomposed into contributions from (1) the orientational correlation of the permanent dipole, which depends on ligand rotational dynamics, (2) the correlation function of the induced dipole whose time dependence, given the constant polarizability tensor, is a measure

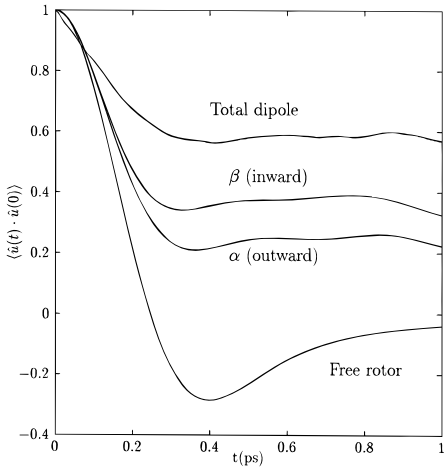

Figure 4. The dipole orientational correlation function computed for the total dipole moment (permanent dipole and induced dipole) and the transition dipole (along the bond) for the α trajectories (outward-pointing distal His) and β trajectories (inward-pointing distal His). The free rotor correlation function is shown for comparison to demonstrate that the CO's motion is hindered. The ligand orientation is significantly more hindered in the β trajectories where there appears to be less free volume in the heme pocket. The β trajectories show better agreement with experiment.

of the correlation of the electric field vector and may have a residual component, and (3) cross correlation between the permanent dipole and induced dipole, which decays rapidly. Figure 4 shows that the decorrelation of the total dipole moment orientation is significantly less than the decorrelation of the permanent dipole (ligand bond) orientation. The permanent dipole orientation may relax by ligand rotation while the relaxation of the induced dipole requires decorrelation in the external electric field as well. In a static electric field, the induced dipole orientational correlation function will have a short time decay, due to the anisotropy of the ligand polarizability, and a residual constant component. In the protein, the electric field is not static. There are fluctuations in the electric field due to oscillations about a well-defined protein structure, tertiary structural rearrangements, and changes in the protonation state of nearby titratable residues. However, there may also be an orientational preference due to the anisotropy of the average charge distribution for the ensemble of conformations corresponding to the folded state.

The induced dipole may add a significant component to the direction vertical to the CO bond vector because the CO has a vertical polarizability comparable to the parallel component of the polarizability matrix $\underline{\alpha}$ and cannot be neglected.[48] Indeed, we found a substantial change of direction of $\vec{\mu}(t)$ away from the CO bond vector. This observation indicates that the CO total dipole moment may not represent the CO bond orientation; however, this will not effect the direction of the transition dipole in this simple diatomic ligand. In Figure 4, the longer time relaxation is not probed. However, in general we expect that the long time scale decorrelation in the total dipole moment of the ligand can provide a measure of the protein and solvent relaxation coupled to the electric field in the heme pocket.

C. Protein Electric Field in the Heme Pocket. In each trajectory, the direction of the electric field measured at the CO center-of-mass is roughly parallel to the heme normal vector. The CO bond vector (pointing from C to O) is not aligned with the electric field; it is more nearly perpendicular to the direction of the field. A possible explanation of this phenomenon is that the dynamics of CO is dominated by van der Waals and field gradient−quadrupolar interactions. Interaction of the small CO dipole moment with the external field is a minor perturbation

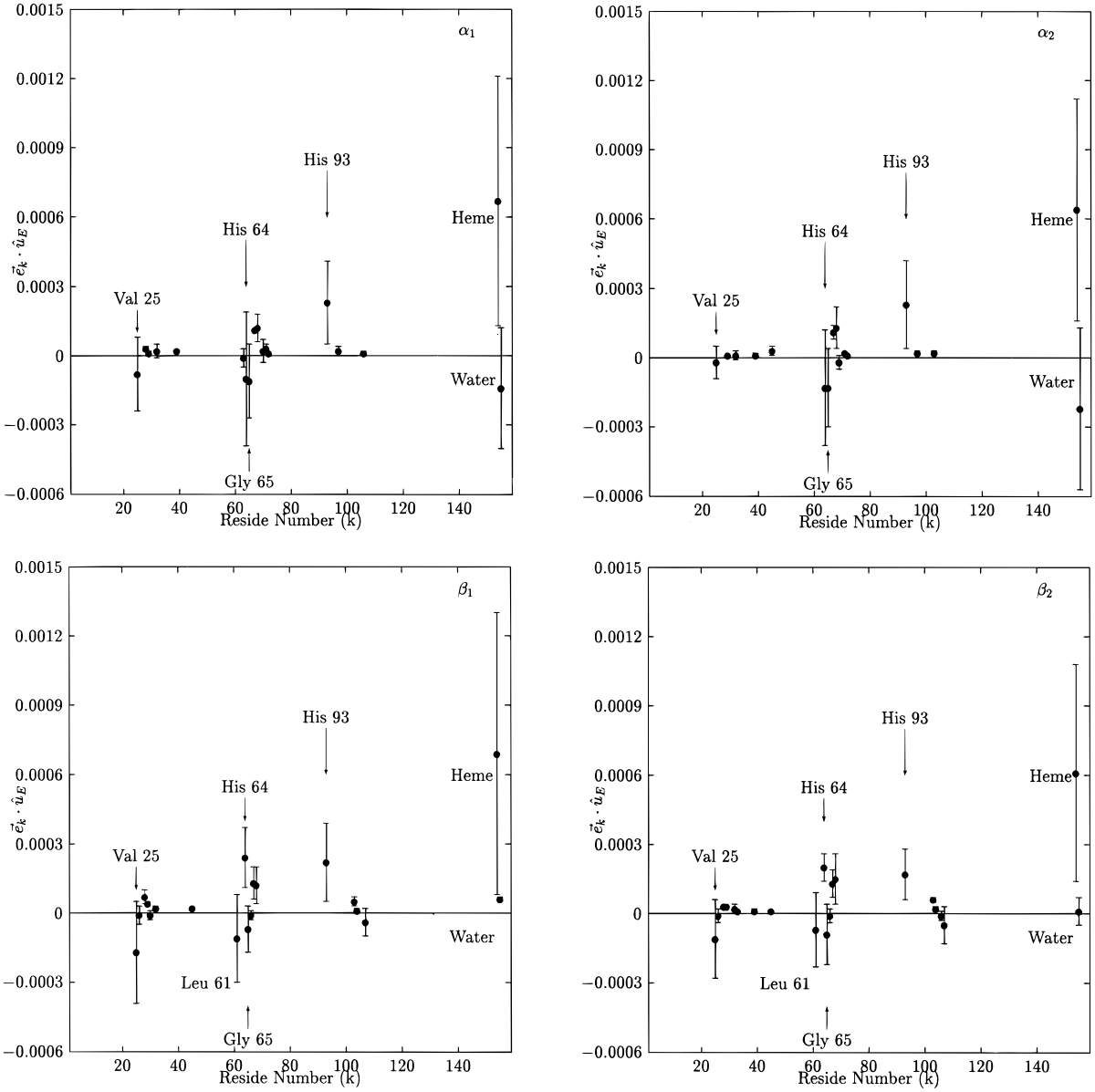

Figure 5. The time-averaged contribution to the external electric field of each residue (●) is shown for the four trajectories used in our study where $\bar{e}_k$ is the time-averaged electric field vector for the *k*th residue measured at the center-of-mass of the CO ligand and projected onto the unit vector of the total electric field of the protein $\hat{u}_E$. The error bars indicate the root-mean-square fluctuation of each contribution.

on the dynamics. This observation was first made in the context of a molecular dynamics simulation study of neat CO liquid.[57] In light of this observation, the three-site CO model was specifically designed to fit the experimental value of the quadrupole moment of CO.

For each individual trajectory, we isolated the components of the electric field by residue (Figure 5). An important and fairly constant contribution (both in magnitude and orientation) to the total electric field is due to the proximal His93 and the heme. In each structure studied, 50% of the magnitude of the electric field is contributed by the proximal His and the heme. During the dynamics, the contributions from the various residues to the electric field are very similar in the α and β trajectories. There are three exceptions. (1) The water solvent makes a significant negative contribution in the α (outward) conformations but not in the β (inward) conformations. The outward distal His conformation allows for closer approach of the ligand to the solvent waters near the heme pocket. (2) Leu61 makes a significant negative contribution in the β trajectories but is a minor contributor in the α trajectories. (3) The distal His64 makes a negative contribution in the α trajectories but a positive contribution in the β trajectories. The magnitude of the contribution of the (neutral) distal His64, which has been emphasized in previous studies, is on the order of 3−10% for the structures studied. However, the *change* in the contribution, between the outward and inward conformations, is significant.

The factor of 2 difference in the average electric field magnitude in the α and β trajectories can be explained by these three contributions (Leu61, His64, and solvent). In the α (β) trajectories, the average total field is 7.9×10^{-4} au (11.8×10^{-4} au); the contribution from Leu61, His64, and solvent is -3.0×10^{-4} au ($+1.7 \times 10^{-4}$ au). Therefore, the contribution from all other groups is 10.9×10^{-4} au (10.1×10^{-4} au), which shows little difference between the electric field seen by the ligand in the outward and inward conformations.

Our calculations indicate that any model of the total electric field for the calculation of frequency shifts must include contributions from a number of groups including the heme, His93, Gly65, Leu61, His64, and solvent. A model of the

(57) Berne, B. J.; Harp, G. D. *Adv. Chem. Phys.* **1970**, *17*, 63.

Table 2. Comparison of the Electrostatic Fields Calculated Using a Simple Point Charge Model of the Protein and Solvent (CHARMM) and a Continuum Electrostatics Model of the Solvent with an Ionic Strength of 600 mM (0 mM) Using UHBD

	CHARMM ($r_c = 9.25$ Å)		CHARMM ($r_c = \infty$)		UHBD	
run	$10^4\|\vec{E}\|$(au)	$\theta_{E\text{-Heme}}$ (deg)	$10^4\|\vec{E}\|$(au)	$\theta_{E\text{-Heme}}$ (deg)	$10^4\|\vec{E}\|$(au)	$\theta_{E\text{-Heme}}$ (deg)
α_1	5.3	119.9	4.7	140.0	8.6 (8.6)	133.3 (133.3)
α_2	7.0	167.3	6.7	150.9	9.5 (9.5)	138.6 (138.5)
β_1	15.8	155.2	12.4	170.0	12.2 (12.3)	161.4 (161.5)
β_2	16.4	163.2	13.6	175.2	14.2 (14.2)	160.5 (160.6)
Mb*CO[a]					11.3 (11.3)	143.7 (143.7)

[a] Computed using the low-temperature X-ray structure.[38]

frequency shift in the ligand based solely on the proximity of the ligand to the distal His64, at neutral pH, is not expected to be accurate for the B-states.

D. Estimates of the Electric Field from a Continuum Solvent Model. The presence of salt and the effect of the solvent ionic strength on the electric field are not accounted for in the explicit point charge model described above. To investigate the effect of ionic strength, we have calculated the electric field in the heme pocket using a continuum model of electrostatic interactions by solving the Poisson−Boltzmann equation using the UHBD program.[58]

The electrostatic potential was first calculated on a coarse grid ($60 \times 60 \times 60$) with 1.5 Å spacing, which contains MbCO and a 30−40 Å region of solvent. The dielectric constant inside and outside MbCO were assigned to values of 1.0 and 78.0, respectively. The ionic strength was set to 600 mM to be consistent with experimental conditions.[9] Using the boundary potential calculated with the coarse grid, the electrostatic charge-field force was calculated on a fine grid ($88 \times 88 \times 88$) with a 0.21 Å spacing centered at the CO center-of-mass.

The probe-accessible dielectric maps were calculated using a probe of radius 1.4 Å. Each atom sphere was assigned a set of 200 surface dots. There are regions inside the protein which are effectively free volume, with no identifiable internal crystallographic waters. Nevertheless, using the standard definitions, these volumes are treated as high dielectric regions. We have modeled these regions of free volume as vacuum and assigned a vacuum dielectric constant of unity (as in the internal protein regions). This differs from similar protocols employed elsewhere.[59] The electrostatic field was computed as the force divided by the charge.

Table 2 presents the value of the electrostatic field at the CO center-of-mass computed by UHBD and CHARMM. We make a few observations based on comparison of the computed electric fields.

(1) The potential without the shift truncation is in good agreement with the continuum electrostatics results.

(2) The electric field experienced by the ligand in the heme pocket during the α trajectories differs from that in the β trajectories in both magnitude and orientation. However, the electric field experienced by the ligand in the two α trajectories is similar (as is the electric field in the two β trajectories) in spite of the fact that the initial configurations for the runs are separated by 100−500 ps of room temperature dynamics. This suggests that at neutral pH there are two dominant conformational substates for the heme pocket region which are well correlated with the value of the χ_2 torsion angle of the distal His64.

(3) The electric field computed for the simulated solution structures is similar in magnitude and orientation to the low-temperature X-ray crystal structure of photolyzed MbCO. This indicates that the simulated solution structures are not qualitatively different, in terms of the electric field seen by the dissociated ligand, from the low-temperature crystal structure. This is consistent with the observed similarity between the heme pocket conformation of the NMR solution structure[35] and the X-ray crystal structure[34] of MbCO and the similarity in the ligand vibrational spectra measured at low temperature[15] and room temperature[9] for Mb*CO.

In the CHARMM calculation, the ionic strength was not taken into account. However, the continuum model, which takes into account the effect of ionic strength in the bulk solvent, shows that the resulting electric field is insensitive to the exact value of the ionic strength in the experimentally measured range (Table 1). This demonstrates that change in the electric field is slight both in magnitude and orientation.

E. A Simple Estimate of the Ligand Vibrational Frequency Shifts. The experimental B-state IR spectrum measured by Lim, Jackson, and Anfinrud has two peaks. They interpret the two peaks as resulting from two conformations of the CO ligand in the binding site which interchange by a rotation beween CO and OC. Furthermore, the ligand is believed to be oriented parallel to the heme plane. We examine this point using a simple model for the static distribution of ligand frequency shifts.

Vibrational frequency shifts in the ligand are induced by van der Waals interactions as well as the external electric field. The van der Waals interactions can be expected to lead to an overall shift in the center of the frequency distribution while the detailed inhomogeneity in the spectra is expected to be primarily induced by the external electric field and electric field gradient.

We use a simple but accurate model of the vibrational frequency shift induced in the CO by an external electric field. Our model is based on the observation that CO has a dipole derivative of approximately −3.1 D/Å.[60] As the CO bond length increases, the dipole moment becomes more negative. Since CO is an anharmonic oscillator, the expectation value of the CO bond length is greater (more positive) in the first excited state than in the ground state. This leads to a dipole moment of $\vec{\mu}_0 = 0.112D\hat{u}_{CO}$ in the ground state (C^-O^+) and $\vec{\mu}_1 = 0.0958D\hat{u}_{CO}$ in the first excited state[61] where $\hat{u}_{CO}$ is the unit vector pointing from the C atom to the O atom. A dipole $\vec{\mu}$ in an electric field $\vec{E}$ has an interaction energy $W = -\vec{\mu}\cdot\vec{E}$. In an external electric field, the vibrational energy levels of the CO will be shifted relative to each other by the difference in interaction energy $\Delta W = -\Delta\vec{\mu}\cdot\vec{E}$ where $\Delta\vec{\mu} = \vec{\mu}_1 - \vec{\mu}_0$. For CO, the difference dipole $\Delta\vec{\mu} = -0.0162\ D\hat{u}_{CO}$ is opposed to the permanent dipole moment of the vibrational ground state.

To first order, the frequency shift can be approximated as $\Delta\nu = \Delta W/h$ or simply

$$\Delta\nu = -{}^1/_h\Delta\vec{\mu}\cdot\vec{E} \qquad (1)$$

(58) Madura, J. D.; Davis, M. E.; Gilson, M. K.; Luty, B. A.; Wade, R. C.; McCammon, J. A. *Rev. Comput. Chem.* **1994**, *5*, 229.

(59) Laberge, M.; Venderkooi, J. M.; Sharp, K. A. *J. Phys. Chem.* **1996**, *100*, 10793.

(60) Chackerian, C., Jr. *J. Chem. Phys.* **1976**, *65*, 4228.

(61) Dubost, H.; Abouaf-Marguin, L. *Chem. Phys. Lett.* **1972**, *17*, 269.

where h is Planck's constant and $\vec{E}$ is the electrostatic field of the protein at the CO center-of-mass. Therefore, if the permanent dipole is aligned with the external electric field, the ground and first-excited state splitting will *increase*, leading to a blue shift. If the permanent dipole is antialigned with the external electric field, the splitting will *decrease* inducing a red shift in the vibrational transition frequency. This effect has been demonstrated in *ab initio* calculations of CO interacting with a variety of small molecules.[27] Similar models of the electric field induced (Stark) vibrational frequency shifts has been applied in the study of double-doped rare gas matrices of CO and a polar molecule[61] and liganded CO in carbon monoxycytochrome c.[59] We employ a slightly modified version of this simple model which leads to a significantly more accurate prediction of the induced frequency shift.

Detailed *ab initio* calculations of frequency shifts in CO induced by an external electric field and electric field gradient have shown that the simple model described above, which ignores electrical polarization effects and underestimates the magnitude of the induced frequency shift, is qualitatively correct but slightly inaccurate.[21,23] (1) The blue and red shifts predicted using a dipole difference of magnitude $|\Delta\vec{\mu}| = 0.0162\ D$ are too small. (2) For the same magnitude of the electric field, the parallel orientation of CO leads to a blue shift which is smaller in magnitude than the corresponding red shift induced in the antiparallel orientation of the CO. Equation 1 predicts that the magnitudes of the induced red and blue frequency shifts are equal.

A slight modification of eq 1 provides us with a reasonably accurate estimate of the frequency shift for the CO ligand in an external electric field. When the angle between the CO and the field is between 0° and 90°, we use a value for the dipole difference of $\Delta\vec{\mu} = -0.0245D\hat{\mu}_{CO}$. When the angle between the CO and the field is between 90 and 180 degrees we use a value of $\Delta\vec{\mu} = -0.030D\hat{u}_{CO}$. Using this approximation, the predicted frequency shifts agree with the *ab initio* values to within roughly 10% for most values of the field up to 0.02 au. The external field at the center-of-mass of the ligand was calculated from a simple sum of the Coulomb field of each atom. A shift function was used in calculating the electrostatic potential and field. Measured fields in the heme pocket rarely exceed 0.01 au, and the frequency shifts are well modeled using the simple approximation. The frequency shifts predicted as a function of angle (between the ligand and field) and field strength are displayed in Figure 6a.

If we assume that the frequency shift is given by eq 1, we can write the spectrum as a probability distribution of the frequency shift

$$P(\Delta\nu) = \langle\delta[\Delta\nu + {}^{1}/_{h}\,|\Delta\vec{\mu}|\,|\vec{E}|\cos\theta]\rangle \qquad (2)$$

where the average is defined as

$$\langle ...\rangle = \int_0^{\pi} \mathrm{d}\theta \sin\theta \int_0^{\infty} \mathrm{d}|\vec{E}|\ ...\ g(\theta,|\vec{E}|) \qquad (3)$$

Here, θ is the angle between the electric field and the CO ligand dipole moment unit vector and $g(\theta,|\vec{E}|)$ is the normalized probability distribution for the occurrence of given values of the angle θ and magnitude of the electric field E. Because the higher order contribution of the field gradient is an even function of ${}^{\pi}/_{2} - \theta$, its inclusion will not change the qualitative features of $P(\Delta\nu)$.

There are two extreme possibilities. (1) If the distribution $g(\theta,|\vec{E}|)$ is peaked at $\theta = 0$ and π, the most likely orientations between the CO and the electric field are parallel and antiparallel. A preponderance of these orientations will lead to two peaks in the distribution $P(\Delta\nu)$ corresponding to the blue and red shifts associated with the CO being parallel or antiparallel to the electric field. (2) If the distribution $g(\theta,|\vec{E}|)$ is peaked at $\theta = {}^{\pi}/_{2}$, there will be a single peak in the distribution of frequency shifts.

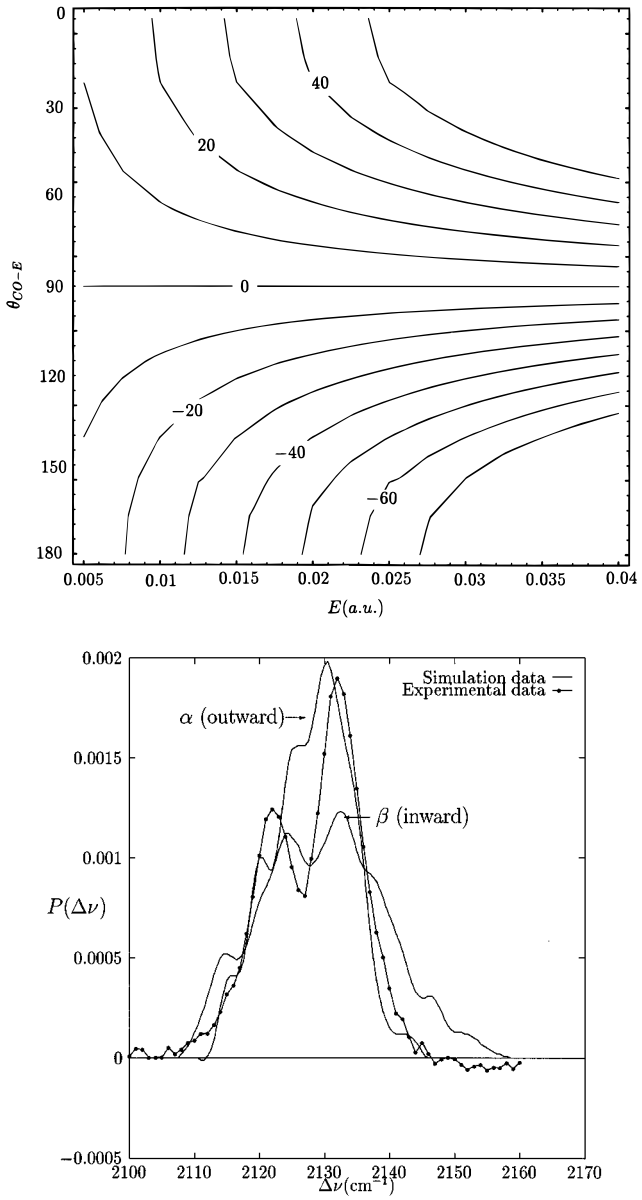

Figure 6. (a) A contour plot showing the frequency shift predicted as a function of the angle $\theta = (\hat{u}_{CO}\cdot\vec{E})/|\vec{E}|$ using our model based on quantum chemical calculations (ref 23). (b) A distribution of the estimated frequency shift induced by the electric field in the heme pocket of the protein for the α and β trajectories. Shown for comparison is the experimental data for ^{12}CO Mb at 283 K.[9] The simulation data is arbitrarily centered to show that the width of the simulated spectrum is in good agreement with the experimental spectrum.

The distribution of the frequency shift is presented in Figure 6b. The width of the probability distribution of the frequency shift for both the α and β trajectories is similar to the width of the experimental spectrum. The distribution of frequency shifts calculated over the β trajectories is slightly broader than that calculated for the α trajectories or the experimental spectrum. The difference between the results for the α and β trajectories could be due to a difference in (a) the distribution of angles of the CO relative to the electric field or (b) the magnitude of the electric field or (c) both. Figure 7 demonstrates that (a) the

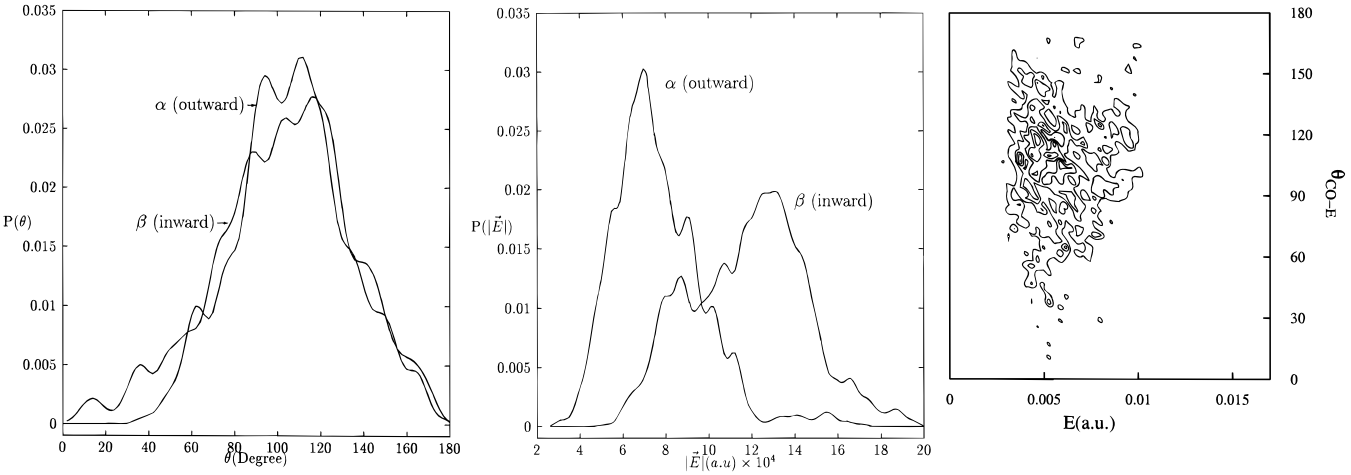

Figure 7. (a) The distribution of the angle of the CO dipole moment relative to the external electric field θ, and (b) the distribution of the magnitude of the electric field $|\vec{E}|$ shown for the α and β trajectories. While the angular distribution of the CO relative to the electric field is similar over the α and β trajectories, the magnitude of the field is significantly greater over the β trajectories. (c) The joint distribution $g(\theta,|\vec{E}|)$ of the angle of the CO dipole moment relative to the external electric field and the magnitude of the electric field. The contour lines indicate regions where there is nonzero probability for locating the CO molecule.

distribution of angles is quite similar in the α and β trajectories while (b) the magnitude of the electric field is significantly larger in the substates sampled over the β trajectory. This is also evident in the data in Table 2.

Figure 3 shows that the electric field is on average approximately perpendicular to the heme plane. Comparison with Figure 7c demonstrates that the ligand is typically nearly perpendicular with the electric field and the heme plane. These data indicate that the second scenario (of the average orientation of the ligand perpendicular to the average orientation of the field) is closest to our simulation data. However, there is a slight splitting into two peaks in the calculated frequency shift distributions for the α and β trajectories. Therefore, our results provide some support for the first limiting case, which corresponds to the interpretation of Lim, Jackson, and Anfinrud. Several other points support this conclusion.

(1) Our estimates of the electric field appear to provide an accurate estimate of the electric field in the Mb heme pocket. We have tested our estimates, derived from the CHARMM force field, with the electric field derived from the solution of the linearized and full Poisson−Boltzmann calculation (using a dielectric constant of 78 in the solvent regions and 1 in the protein regions and in the heme pocket) and found them to be in excellent agreement.

(2) The data of Alben *et al.*[15] shows the existence, in the crystal, of B-states similar to those seen at room temperature in solution.[9] This implies that the orientation of the protein electric field in the heme pocket should be similar in the solution and the crystal. We have calculated the electric field for the myoglobin low-temperature X-ray crystal[38] structure and found that the electric field is consistent in both direction and magnitude with the field measured in our simulation.

(3) Interconversion between the B_1- and B_2-states is observed[15] at 20.1 K with a barrier to interconversion (0.9 kcal/mol) comparable to that estimated by Lim, Jackson, and Anfinrud (1.2 kcal/mol) from the decorrelation of the ligand dipole orientational correlation function at 283 K.[9] The simulated rotational relaxation of the dipole orientation is in good agreement with the experimentally derived value. This is further evidence that the ligand orientation and dynamics is well modeled by the simulations.

It is possible that there is an important interaction between the CO and protein responsible for inducing the ligand vibrational frequency shift which is not accounted for in our model. There is evidence that the B_1-band shifts nonexponentially in time up to 10 ns while the B_2 band is stabilized a short time after photolysis.[19] Therefore, if the B_1- and B_2-states do differ simply by their angular orientation, there must be an important interaction between the protein and the B_1-state which is absent in the B_2-state. One possibility is an interaction between the heme Fe and ligand O.[19] However, there is no direct evidence that our model for the origin of the frequency shift is lacking.

IV. Conclusions

We have drawn a number of conclusions from our study relating to the topics described in the Introduction.

(1) The short-time ligand dynamics at room temperature is modeled reasonably well. There is good agreement between theory and experiment for the dipole orientational correlation function. A previous simulation based on a stochastic boundary simulation of the photolyzed state showed similar agreement with experiment.[27] This indicates that for the ligand reorientational dynamics the stochastic boundary simulation agrees well with the results of the fully solvated protein.

(2) Our study indicates that the largest single contribution to the electric field in the heme pocket is due to the proximal His and the heme itself. A number of studies have assumed that the electric field is primarily or entirely due to the distal histidine. We find that at pH 7 the (neutral) distal His is a significant but minor contributor to the field experienced by the dissociated (B-state) ligand.

(3) The conformation of the distal His, described in this study by the value of its χ_2 torsion angle, plays an important role in determining the magnitude and direction of the field that is experienced by the ligand. The electric field is inhomogeneous, and the particular value of the field will depend on the position of the ligand in the pocket. The conformational state of the His appears to determine the regions of the pocket accessible or most favorable to the ligand.

(4) Continuum electrostatics calculations, which account for the ionic strength of the solvent, agree well with continuum electrostatics calculations which ignore the ionic strength (Table 1). This indicates that the electric field in the heme pocket is largely insensitive to the value of the ionic strength for the range of ionic strength explored.

(5) The width of the simulated distribution of frequency shifts induced in the ligand is in good agreement with the existing

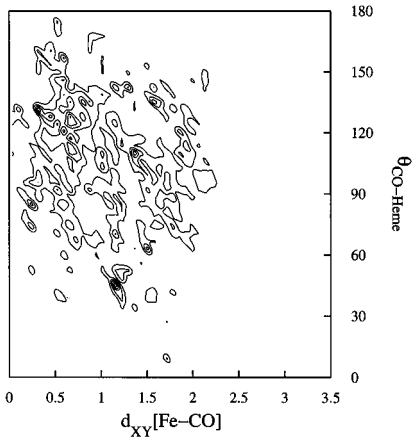

Figure 8. The joint distribution $f(\theta,d_{xy}(Fe-CO))$ of the angle of the CO dipole moment relative to the heme normal θ and the distance of the projection onto the heme plane of the CO ligand bond center to the heme iron $d_{xy}(Fe-CO)$. The contour lines indicate regions where there is nonzero probability for locating the CO molecule.

experimental spectra. This implies that the magnitude of the electric field in the heme pocket is accurately modeled. It has been proposed that the two B-state lines correspond to parallel and antiparallel orientations of the CO.[9] Within our model of the frequency shift, it would be necessary to have the electric field on average in the plane of the heme to induce two lines in the ligand spectrum. Our simulations predict a field which is on average parallel to the heme normal. The simulated spectra show some "split" structure but lack two distinct lines associated with specific "substate" conformations of the dissociated ligand.

The induced dipole moment in the ligand is significant and can strongly influence the orientation of the total dipole moment. The induced dipole moment decorrelates slowly compared with the time scale for ligand rotation. This contribution to the orientational correlation function may serve as an important measure of protein relaxation. We note that this long-lived induced dipole is qualitatively different from previous studies of collision induced dipoles where the induced dipole typically relaxes rapidly compared with the rate of molecular reorientation.

(6) The distribution of the angle between the CO bond vector and the heme normal vector was investigated. The results indicate that at room temperature the CO molecule is loosely confined in a "layer" parallel to the heme plane which on average has a width of 2−2.5 Å and a thickness of 0.5−1.0 Å. The vertical distance of the "layer" to the heme plane or binding site is much larger than the binding distance of 4.0−6.0 Å. This "plane" is located between the B- and C-rings.

(7) Finally, let us examine the distribution of CO in the heme pocket of Mb generated by our simulation and ask if there is significant bias away from the expected transition state geometry for CO rebinding. Figure 8 shows that there is a strong correlation between the angle of the CO ligand relative to the heme plane and the position of the ligand relative to the heme Fe. When the ligand moves beneath the heme Fe atom, it is not observed to be at a *nearly* perpendicular angle which is assumed to be a necessary transition state geometry for rebinding to the heme. Therefore, it appears that while the ligand is not strongly restricted to a binding site, it is uncommon for the ligand to move into the transition state geometry necessary for rebinding.

In the transition state geometry, the Fe−C distance is expected to be longer than the equilibrium geometry. In the transition state, there may well be a significant steric repulsion with the heme pocket making a ligand configuration normal to the heme plane energetically unfavorable. It is possible that steric repulsion raises the energy of the transition state for CO rebinding relative to the equilibrium bound state. This would lead to a smaller rate of rebinding in the protein relative to the protoheme.

Acknowledgment. We thank Charles L. Brooks, III, for providing us with the unpublished 1.5 ns equilibrium deoxymyoglobin trajectory which made our simulation study possible. We are grateful to Philip A. Anfinrud for many helpful suggestions. J.E.S. gratefully acknowledges the Petroleum Research Fund of the American Chemical Society (30601-AC6) and the Alfred P. Sloan Foundation for support and the National Science Foundation for support (CHE-9306375) and computational resources at the Pittsburgh Supercomputing Center (CHE-930040P) and the National Center for Supercomputing Applications (CHE-950015N).

JA9608252